U.S. DEPARTMENT OF THE INTERIOR

U.S. GEOLOGICAL SURVEY

CHARACTERIZATION OF SECONDARY MINERALS FORMED AS THE RESULT OF WEATHERING OF THE ANAKEESTA FORMATION, ALUM CAVE, GREAT SMOKY MOUNTAINS NATIONAL PARK, TENNESSEE

by

Marta J.K. Flohr[1], Roberta G. Dillenburg[1], and Geoffrey S. Plumlee[2]

Open-File Report 95-477

[1] U.S. Geological Survey
National Center, MS 959
Reston, VA 22092

[2] U.S. Geological Survey
Denver Federal Center, MS 973
Denver, CO 80225

1995

CONTENTS

ILLUSTRATIONS

TABLES

Introduction

The environmental impact of weathering of both natural and man-made exposures of the Anakeesta Formation in the Great Smoky Mountains National Park (GSMNP), North Carolina and Tennessee (Fig. 1) has been of concern to the National Park Service for a number of years. Weathering of the iron-sulfide-bearing metamorphic rocks that comprise the Precambrian Anakeesta Formation has produced acid drainage in parts of the park. Exposures of Anakeesta rocks at Alum Cave (Fig. 1), which is along the heavily hiked Alum Cave Trail, has raised health concerns of a different nature. Alum Cave is not a real cave, but rather a bluff that has been eroded to produce a cave-like overhang. Within this structure, the Anakeesta phyllite is protected from precipitation, but low volumes of groundwater seep along planes of schistosity and alter the rock. Fine-grained soluble secondary minerals form by the evaporation of this acidic metal-bearing groundwater. This fine-grained material sloughs off the formation and is incorporated into the soil below. As hikers walk through the soft dry soil beneath the Alum Cave overhang, significant amounts of dust are raised that have a bitter "alum" taste (hence, the name "Alum" Cave), which has been attributed to the presence of the secondary minerals derived from the phyllite. Hiker traffic through the area is heavy because Alum Cave is both a popular destination for day hikers and it lies along the trail that leads to Le Conte Lodge, which is located on the west slope of Mount Le Conte and which is only accessible by foot. The concern of possible adverse health effects on hikers that walk through the soil and breathe the dust at Alum Cave has been raised by the National Park Service.

The purpose of this study was to identify and chemically characterize the secondary minerals that form from the Anakeesta phyllite at Alum Cave, so that their potential environmental and (or) health impact could be further assessed. This mineralogical study compliments leaching experiments currently in progress by one of the authors (G.S.P.) on samples from Alum Cave. In addition to specifically addressing the formation and stability of the secondary minerals at Alum Cave, these studies will contribute to a better understanding of the processes that lead to alteration of Anakeesta rocks and to the generation of acidic drainage within the GSMNP. A brief summary of the environmental problems caused by the weathering of Anakeesta rocks is given in the following section.

Geological Setting and Environmental Considerations

The Anakeesta Formation is composed of units of slate, phyllite, and schist that are interbedded with sandstone layers and that crop out in the central and south-central part of the GSMNP (King and others, 1968). The argillaceous metasedimentary rocks contain carbonaceous material or graphite, depending on the temperatures attained during metamorphism, and the iron sulfide minerals, pyrrhotite and (or) pyrite. Detailed descriptions of the geology and mineralogy of the Anakeesta Formation were provided by Hadley and Goldsmith (1963), King (1964), King and others (1968), Mohr and Newton (1983), and Mohr (1984). Weathering of the naturally exposed sulfide-bearing rocks contributes to acid drainage and elevated metal concentrations in Walker Camp Prong and Alum Cave Creek (Herrmann and others, 1979) in the central part of the park, near Newfound Gap (Fig. 1). High concentrations of certain metals (Fe, Al, Zn, Mn, and Mg) in the surficial sediments of Fontana Lake, about 27 km to the southwest of Newfound Gap, were attributed to weathering of Anakeesta rocks in part of the drainage area that feeds the lake (Abernathy and others, 1984). Elevated Cu concentrations in two of the Fontana Lake sediment samples were attributed to weathering of Cu mineralized rocks in the area.

Construction of U.S. Highway 441 in the mid 1960s led to extensive exposure of the Anakeesta Formation to weathering. The Anakeesta Formation was exposed in roadcuts in the central part of the park, in the area of Newfound Gap, and material removed during the road construction was used as road fill (Bacon and Maas, 1979). High mortality rates of brook trout and salamander were observed in streams that drain areas of the road construction and immediately below the road fill in Beech Flats Creek (Fig. 1). These high mortality rates were attributed to a decrease in the stream's pH from normal values of about 6.5 to 7 to a pH of 4.5 and an increase in the metal content of the waters compared to preconstruction levels (Bacon and Maas, 1979; Herrmann and others, 1979; Trumpf and others, 1979; Mathews and others, 1982; Kucken and others, 1994). Bacon and Maas (1979) reported that Mn concentrations increased from an undetectable level to >250 ppb and that Zn concentrations increased from 6 to nearly 200 ppb in the area where Beech Flats Creek flows through the U.S. 441 road cut fill area. Herrmann and others (1979) reported that Al concentrations increased from <0.01 ppm to 6.9 ppm and that sulfate concentrations increased from 0.59 ppm to 132 ppm in the affected segments of Walker Camp Prong and Beech Flats Creek.

The Anakeesta Formation and the surrounding Thunderhead sandstone (Fig. 1) do not have the capacity to buffer the acidity of drainage waters in the region around Newfound Gap. Carbonate minerals are a very minor constituent of the Thunderhead sandstone (Hadley and Goldsmith, 1963). Thin dolomitic beds, which contain 40-95 vol. % dolomite, occur in the Anakeesta Formation to the north of Newfound Gap (Hadley and Goldsmith, 1963). Probably because of the limited exposure of these dolomitic beds, dissolution of dolomite exercises only limited and local control in buffering the acidity of the drainage waters.

Acid drainage is caused by the oxidation of sulfide minerals such as pyrite and pyrrhotite, which occur in the rocks of the Anakeesta Formation. Nordstrom and others (1979) summarized the chemical reactions that involve the oxidation of pyrite. The initial oxidation of pyrite produces ferrous iron ions and sulfur. Sulfate and ferric iron ions are produced with further oxidation. The production of ferric iron leads to further oxidation of pyrite, with the ferrous iron produced being oxidized to ferric iron by the acidophilic iron-oxidizing bacterium *Thiobacillus ferroxidans*. Similarly, the oxidation of pyrrhotite also leads to acidic conditions, but pyrite produces more acid per mole than pyrrhotite (Nicholson, 1994). The difference in the acid generating capabilities of the two Fe-sulfide minerals is attributed to the greater S content of pyrite (Nicholson, 1994).

Only a limited number of analyses of Anakeesta rocks are reported in the literature. Mohr and Newton (1983) reported 0.01 - 1.83 wt. % S in Anakeesta schists from an outcrop about 13 km south of Newfound Gap, consistent with the 1.3 wt. % S reported by Hadley and Goldsmith (1964) in pyritic argillite from an outcrop exposed in the eastern part of the Anakeesta Formation shown in Figure 1. The limited data indicate a range in the amount of sulfide minerals present in the different lithologies of the Anakeesta. More detailed study of the Anakeesta rocks is required to better correlate their sulfide content with the acid drainage problems summarized above.

Samples and Methods of Analysis

Samples were collected by one of us (G.S.P.) from a sheltered part of Alum Cave and three were chosen for detailed characterization. The samples consist of thin sheets and fragments of the Anakeesta phyllite that have been extensively replaced and encrusted by a variety of secondary minerals. A given sample does not consist of a single piece of

rock, but rather small fragments of phyllite encrusted by the secondary minerals and of encrustations, some of which contain pieces of phyllite, but some of which do not. A striking macroscopic replacement texture occurs as thin sheets of phyllite, typically < 1 mm thick, interlaminated with or embedded within somewhat porous thicker layers of secondary minerals.

Minerals were identified by X-ray powder diffraction (XRD) and their chemical compositions qualitatively characterized by use of the X-ray energy-dispersive analysis system (EDS) on the JEOL JSM-840 scanning electron microscope (SEM). Selected minerals were analyzed on the SEM using a standardless software analysis routine that uses a ZAF correction procedure (Princeton Gamma-Tech, Inc., 1994). These analyses are regarded as semi-quantitative, based on analyses of well-characterized mineral standards. Polished slabs and thin sections of the Anakeesta phyllite also were examined using the petrographic microscope. These phyllite samples were free of nearly all secondary phases, the exception being the Fe-rich crusts that are described below.

Standard XRD procedures were used. Samples for XRD were hand picked under a binocular microscope. Because the secondary minerals rarely occur as discreet monomineralic aggregates or segregations and because the minerals are typically fine grained, it was usually not possible to obtain pure separates of individual phases. All samples were ground in acetone and prepared as either smear mounts or slurries on quartz plates. Nickel filtered CuKα X-ray radiation was used. The X-ray unit was operated at 40 kV and 30 mA. X-ray diffraction patterns were obtained as either scans, typically run at 1° 2θ per minute from 70° to 4° 2 , or as step scans run at 100 steps per degree 2 , with a count time of 1.2 seconds per step.

Polished samples of Anakeesta phyllite were examined by SEM to obtain semi-quantitative analyses of the major rock-forming minerals and to help identify and qualitatively characterize the compositions of accessory phases found by optical examination, but whose low abundances precluded detection by XRD. Fragments of encrustations of the secondary minerals from each of the three samples studied were also examined by SEM. As best as possible, SEM samples were chosen to be correlated with XRD samples of the same phases. Additional samples of secondary minerals were examined by SEM to determine if phases not detected by XRD were present and to qualitatively assess the compositional diversity of each secondary mineral. The SEM was operated at an accelerating voltage of 20 kV and a specimen current of about 1 to 2 nA. All samples were coated with a conductive carbon film under vacuum, prior to examination in the SEM.

Mineralogy of the Anakeesta Phyllite

The samples of the Anakeesta phyllite examined as part of this study are composed of quartz, muscovite, paragonite, chlorite, and accessory garnet, rutile, pyrite, pyrrhotite, allanite, monazite, apatite, and zircon (Table 1). Xenotime was tentatively identified, based on SEM-EDS. Fine black particles that are < 1-2 μm across and that are disseminated throughout the phyllite are presumed to be graphite or noncrystalline carbonaceous material, as has been previously reported in schist, phyllite, and slate from the Anakeesta Formation (Hadley and Goldsmith, 1963; King and others, 1968; Mohr and Newton, 1983). Tourmaline, which had been reported to occur in Anakeesta rocks (Mohr and Newton, 1983), was not observed in this study. Qualitative SEM-EDS analysis and standardless analysis indicate that the garnets are rich in the almandine ($Fe_3Al_2Si_3O_{12}$) and spessartine ($Mn_3Al_2Si_3O_{12}$) components and contain only minor Mg and Ca. Chlorite is

intermediate in composition with respect to Mg and Fe contents and contains minor Mn (<1 wt. % MnO). These data are consistent with the electron microprobe analyses of garnet and chlorite from Anakeesta rocks that were reported by Mohr and Newton (1983).

Mineralogy of Efflorescent Salts and Oxidation Coatings

A variety of secondary minerals that form encrustations and which replace the Anakeesta phyllite were identified. The chemical and textural characteristics of the minerals and their ideal formulas are given in Table 2. The list (Table 2) is dominated by hydrated sulfate minerals. The sulfate minerals are efflorescent salts, as they formed when acidic metal-bearing groundwater that seeped through the phyllite evaporated. The intimate association of the various secondary salts is illustrated in Figures 2a and 2b. Oxidation coatings are not as common or as massive as the encrustations of efflorescent salts. These thin oxidation coatings may be sparsely or massively encrusted by sulfate minerals (Figs. 3a, 3b, 3c). A summary of the minerals identified in each of the three samples examined is given in Table 3.

Development of the secondary minerals takes several forms. As described above, one texture consists of thin sheets of phyllite interlaminated with or embedded within layers of secondary minerals. In melanterite- and rozenite-rich samples, white-to-cream layers rich in melanterite ± rozenite commonly occur in contact with the phyllite, with layers rich in waxy to needle-like halotrichite adjacent to the Fe-sulfate-rich layers. Aggregates of halotrichite were also found embedded in melanterite-rozenite layers. Secondary minerals also form fracture fillings within phyllite. Thin clear plates and sheets of gypsum, finely crystalline green-yellow masses of slavikite, bundles of halotrichite needles, and goethite are common fracture fillings. Other fragments of phyllite are simply encrusted with the secondary minerals. Copiapite (Fig. 4a), halotrichite, melanterite, and rozenite are the minerals that form relatively thick encrustations.

Halotrichite and copiapite can form nodular encrustations that may be zoned. Copiapite nodules may contain cores of halotrichite and slavikite, suggesting successive development of the secondary minerals. Halotrichite-rich encrustations may be zoned with respect to color that reflects the relative abundance of minor elements in the halotrichite (Table 2). Copiapite was never observed in the interior of such encrustations. The Mg-sulfate minerals were found only on the underside of halotrichite encrustations.

The identifications of the two Mg-sulfate minerals, epsomite and starkeyite, are somewhat tentative. SEM examination confirmed the presence of two morphologically distinct minerals that are rich in Mg and S. Clean separates could not be obtained for XRD analysis and neither phase is abundant. XRD patterns of the mixtures that contain each of these phases included a relatively few number of peaks that are consistent with epsomite and starkeyite.

Iron-rich, macroscopically smooth, thin dark red crusts occur on phyllite surfaces and on fracture surfaces. The crusts have a variety of morphologies (Table 2) and commonly are sparsely (Figs. 3a, 3b) to abundantly (Fig. 3c) encrusted by a mineral, phase A (Table 2), that is tentatively identified as a member of the alunite mineral group, possibly hydronium jarosite. The red crust is not abundant and is thin, making it difficult to separate it from the underlying phyllite. XRD patterns of crust-rich samples yielded weak patterns with peaks that were attributed to some of the phyllite minerals, sparse and weak peaks that corresponded to goethite, and peaks that were consistent with minerals of the alunite group. SEM-EDS qualitative and standardless analysis of phase A indicated only Fe and S were present and in a ratio that approached that of Fe:S in hydronium jarosite,

although Fe was slightly higher than expected in hydronium jarosite. Some of the Fe may be contributed from the underlying Fe-rich crust; given the small grain size of phase A, the activation volume of the electron beam probably exceeds the size of the individual grains. The morphology of phase A is also consistent with hydronium jarosite. At this time the alunite-group peaks in the XRD pattern are attributed to phase A, and phase A is tentatively identified as hydronium jarosite based on its lack of K and (or) Na and the absence of any other alunite group mineral, as indicated by SEM examination. The red crusts are identified as goethite, based on the presence of weak and somewhat broad goethite peaks in the XRD patterns; the weak, broad peaks indicate that the goethite is poorly crystalline. The red crusts were observed in cross section in polished samples of phyllite. The crusts are generally less than 20-30 μm thick and are compositionally zoned. Higher S was found in the outer surface of the crusts compared to the interior. Aluminum, P, and Si were detected by SEM-EDS in both the outer and inner zones of the crusts, but no consistent correlation between the relative concentrations of these three elements with zoning was found. Ionic substitution of various cations and sorption of anions has been studied in both natural and synthetic samples of goethite. Phosphate (Parfitt and others, 1975) and sulfate (Turner and Kramer, 1991) are adsorbed on goethite, whereas Al (Schulze and Schwertmann, 1984) substitutes for Fe in the goethite structure. The role of Si is not clear; Deer and others (1992) reported that the SiO_2 commonly reported in analyses of goethite is due to admixture and impurities, but Chapman and others (1983) concluded that Si was adsorbed on amorphous $Fe(OH)_3$ and this may be the case for poorly crystalline goethite as described here.

Goethite also occurs as grains embedded in crusts of other secondary minerals (Table 2), suggesting that there are two generations of goethite. Goethite grains yielded relative strong XRD patterns compared to those of goethite that forms the red crusts, indicating that the grains are better crystallized material. Sulfur was not detected on fresh fracture surfaces of goethite grains, but was detected on exposed surfaces of the same grains, which are also partly encrusted by phase A.

A fine orange to yellow-orange "powder" is found on phyllite surfaces and is observed as a fine dusting on surfaces of gypsum plates found on phyllite fracture surfaces. Phase A is a major constituent of the powdery material. Lesser amounts of the other secondary minerals and flakes of phyllite are also present.

Discussion and Conclusions

Mineralogy

The association of some or all of the hydrated sulfate minerals described herein (Table 2) with each other has been reported from a number of other occurrences. These minerals form as oxidation products on pyritic coal seams (e.g., Zodrow, 1980; Weise and others, 1987; Young and Nancarrow, 1988), as the secondary sulfates formed during oxidation of sulfide deposits (e.g., Kyriakopoulos and others, 1989), and are associated with altered pyritized phyllites and shales (e.g., Sclar, 1961; Makovický and Streško, 1967; Cody and Biggs, 1973). Palache and others (1951) detailed numerous occurrences.

Neither jarosite ($KFe_3[SO_4]_2[OH]_6$), natrojarosite ($NaFe_3[SO_4]_2[OH]_6$), or any of the other alkali-bearing sulfates that have been reported as secondary minerals from acid mine drainage areas (Alpers and others, 1994) were identified in the GSMNP samples. If muscovite and (or) paragonite were altered, then one or more alkali-bearing secondary phases might be expected. If the tentative identification of hydronium jarosite is correct, its presence, rather than that of jarosite or natrojarosite, suggests that either hydronium

jarosite is stable and precipitates under different conditions than the alkali-bearing jarosites or that muscovite and (or) paragonite are not weathering and releasing K and Na into solution. Brophy and Sheridan (1965) and Ripmeester and Ratcliffe (1986) reported that hydronium jarosite, rather than jarosite, forms from only alkali-poor solutions. Rapid weathering of pyrite, relative to silicate minerals that could be sources of alkalis, was also suggested as a factor governing the formation of hydronium jarosite (Shayan and Lanucki, 1984; Ripmeester and others, 1986). A similar situation may exist for ammoniojarosite ($NH_4Fe_3[OH]_6[SO_4]_2$), which was found (rather than K- or Na-jarosite) as a coating on gypsum that formed fracture coatings within micaceous shale (Odum and others, 1982). The acidity of the waters from which the various jarosite minerals form is probably also an important factor; different compositional end members may be stable over different ranges of pH (for example, Bigham [1994] summarized several studies which indicated that K-jarosite is not stable at pH > 3-3.5). Additional studies are needed to better define the conditions of formation and stability of some of the jarosite minerals.

The relative abundance of the secondary minerals is different among the three samples studied (Table 3), which may reflect slightly different microgeochemical environments. For example, there are differences in the relative abundances of metamorphic minerals in the three phyllite samples and, hence, slight differences in the bulk composition of each phyllite. Also, given the extensive replacement of phyllite, it is apparent that the secondary minerals developed over a prolonged period of time. Different mineralogies may, in part, reflect slightly different conditions (pH, exposure to air, humidity) during progressive development of the secondary minerals. For example, copiapite was identified in only one sample, and in that sample melanterite is apparently absent and rozenite is not as abundant as in the other two samples. Nordstrom (1982) suggested that copiapite may form from melanterite, a reaction that requires lower pH and more oxidizing conditions than those under which melanterite forms. Mg-sulfate minerals, tentatively identified as epsomite and starkyite, were found only in the sample in which Mg-rich halotrichite appears to be relatively common. It must also be noted that, given the fine-grained nature of the secondary minerals and their propensity to be intimately associated with one another, it is possible that a given mineral, present in only minor amounts, may not have been identified in a particular sample (for example, the apparent lack of alunogen in one sample and gypsum in another, Table 3).

The compositions of the efflorescent salts and the Fe-rich oxidation crusts that form on the Anakeesta phyllite reflect the compositions of the metamorphic minerals that are found in the phyllite. The paragonite, muscovite, chlorite, and garnet are likely sources for Al. Garnet also provides Ca to form gypsum and Fe, Mg, and Mn that is found in several of the secondary phases (Table 2). Chlorite is a source of Mg, Fe, and Mn. Iron is also derived from the weathering of pyrrhotite and pyrite, as is S. Phosphorous, found in the Fe-rich crusts, goethite, and copiapite, is derived from the weathering of one or more of the phosphate minerals, most likely apatite. Monazite and xenotime are relatively resistant to weathering. No rare earth elements, which would be derived from monazite and xenotime, were detected in the secondary minerals by SEM-EDS, but concentrations may be below the detection limit. Zinc was not detected in any of the metamorphic minerals examined in this study, but it may be below the detection limit of the SEM-EDS. Minor amounts of Zn were found in some halotrichite (Table 2) from Alum Cave, which suggests that Zn is present in at least trace quantities in one or more minerals in the phyllite. A more detailed study of the Anakeesta phyllite from Alum Cave, including the collection of quantitative mineral analyses by electron microprobe, is required to identify the source of Zn in the halotrichite.

Environmental and health considerations

The development of secondary minerals, such as those described in this report, require either prolonged dry periods to form or a sheltered area that is protected from precipitation, such as Alum Cave. If exposed to precipitation, the salts would rapidly dissolve and generate acidic metal-bearing waters that may degrade water quality of local streams. Preliminary results of leaching experiments show that the salts rapidly dissolve in distilled water, with a resultant drop in pH and an increase in the conductivity of the leachate water. Even exposure to high humidity conditions leads to rapid dissolution. For example, halotrichite-rich encrustations and rozenite/melanterite efflorescences on phyllite surfaces were observed to dissolve by simply exposing the minerals to a high relative humidity environment in the laboratory. Reprecipitation of the solid phases occurred upon exposing the samples to the normal room humidity. The spontaneous formation of hydrated sulfates on pyrite-bearing rocks and the hydration/dehydration of Fe-sulfate minerals under various "normal" laboratory conditions also has been documented by other workers (e.g., Weise and others, 1987 and references therein). The sulfate minerals copiapite, melanterite, rozenite, gypsum, epsomite, and alunogen are considered among the most soluble of the secondary minerals formed as the result of acid drainage, whereas members of the alunite-jarosite group, such as hydronium jarosite, are considered less soluble (Alpers and others, 1994). The results of this study show that the highly soluble secondary salts are more abundant products of alteration of Anakeesta phyllite than the less soluble minerals and that they host a variety of elements (Al, Fe, Mn, Mg, P, Zn, S). These elements are the same as those that were reported to be present in higher than background concentrations in streams affected by acid drainage due to weathering of the Anakeesta rocks, as summarized above. Development of crusts of soluble efflorescent salts on exposed Anakeesta rocks does not occur because of the relatively high rainfall and periods of high relative humidity in the region. Rather than forming secondary minerals as at Alum Cave, the elements leached from the rocks during alteration are washed into the local creeks.

It is not known if the incorporation of the secondary minerals formed at Alum Cave into the soils below the cave overhang causes any adverse health effects to hikers. The identification and characterization of the minerals study provides some of the data needed to assess possible health problems, but such an assessment is beyond the scope of this study.

References Cited

Abernathy, A.R., Larson, G.L., and Mathews, R.C., Jr., 1984, Heavy metals in the surficial sediments of Fontana Lake, North Carolina: Water Research, v. 18, p. 351-354.

Alpers, C.N., Blowes, D.W., Nordstrom, D.K., and Jambor, J.L., 1994, Secondary minerals and acid mine-water chemistry: *in* Jambor, J.L. and Blowes, D.W., eds., Environmental geochemistry of sulfide mine-wastes, Mineralogical Association of Canada, p. 247-270.

Bacon, J.R., and Maas, R.P., 1979, Contamination of Great Smoky Mountains trout streams by exposed Anakeesta Formations: Journal of Environmental Quality, v. 8, p. 538-543.

Bigham, J.M., 1994, Mineralogy of ochre deposits formed by sulfide oxidation: *in* Jambor, J.L. and Blowes, D.W., eds., Environmental geochemistry of sulfide mine-wastes, Mineralogical Association of Canada, p. 103-132.

Brophy G.P., and Sheridan M.F., 1965, Sulfate studies IV: The jarosite-natrojarosite-hydronium jarosite solid solution series: American Mineralogist, v. 50, p. 1595-1607.
Chapman, B.M., Jones, D.R., and Jung, R.F., 1983, Processes controlling metal ion attenuation in acid drainage streams: Geochimica et Cosmochimica Acta, vol. 47, p. 1957-1973.
Cody, R.D., and Biggs, D.L., 1973, Halotrichite, szomolnokite, and rozenite from Dolliver State Park, Iowa: Canadian Mineralogist, v. 11, p. 958-970.
Deer, W.A., Howie, R.A., and Zussman, J., 1992, An introduction to the rock-forming minerals, 2nd edition, Longman, UK, 696 p.
Fleischer, M., and Mandarino, J.A., 1991, Glossary of mineral species, The Mineralogical Record Inc., Tucson, 256 p.
Hadley, J.B., and Goldsmith, R., 1963, Geology of the eastern Great Smoky Mountains, North Carolina and Tennessee: U.S. Geological Survey Professional Paper 349B, 118 p.
Herrmann, R., Morgan, E.L., and Green, R.L., 1979, Aluminum precipitation, Beech Flats and Walker's Prong Creeks, Great Smoky Mountains National Park: *in* Lin, R.M., ed., Proceedings of the First Conference on Scientific Research in the National Parks, U.S. Department of the Interior, National Park Service Transactions and Proceedings Series Number 5, v. II, p. 715-718.
King, P.B., 1964, Geology of the central Great Smoky Mountains, Tennessee: U.S. Geological Survey Professional Paper 349C, 148 p.
King, P.B., Neuman, R.B., and Hadley, J.B., 1968, Geology of the Great Smoky Mountains National Park, Tennessee and North Carolina: U.S. Geological Survey Professional Paper 587, 23 p.
Kucken, D.J., Davis, J.S., Petranka, J.W., and Smith, C.K., 1994, Anakeesta stream acidification and metal contamination: Effects on a salamander community: Journal of Environmental Quality, vol. 23, p. 1311-1317.
Kyriakopoulos, K.G., Stamatakis, M.G., and Mitsis, J.P., 1989, Copper- and cobalt-rich hydrous sulphate aggregates from a disused sulphide mine in the Plaka, Laurium area, Greece: Annales Geologuiques des Pays. Hellenique, v. 34, p. 77-88.
Makovický, E., and Streško, V., 1967, Slavikite from Medzev near Košice, Czechoslovakia: Tscherm. Mineral. Petrog. Mitt., v. 12, p. 100-107.
Mathews, R.C., Jr., and Morgan, E.L., 1982, Toxicity of Anakeesta Formation leachates to shovel-nosed salamander, Great Smoky Mountains National Park: Journal of Environmental Quality, v. 11, p. 102-106.
Mohr, D.W., 1984, Zoned porphyroblasts of metamorphic monazite in the Anakeesta Formation, Great Smoky Mountains, North Carolina: American Mineralogist, v. 69, p. 98-103.
Mohr, D.W., and Newton, R.C., 1983, Kyanite-staurolite metamorphism in sulfidic schists of the Anakeesta Formation, Great Smoky Mountains, North Carolina: American Journal of Science, v. 283, p. 97-134.
Nicholson, R.V., 1994, Iron-sulfide oxidation mechanisms: laboratory studies, *in* Jambor, J.L., and Blowes, D.W., eds., Environmental geochemistry of sulfide mine-wastes, Mineralogical Association of Canada, p. 163-183.
Nordstrom, D.K., 1982, Aqueous pyrite oxidation and the consequent formation of secondary iron minerals, *in* Kittrick, J.A., Fanning, D.S., and Hosner, L.R., eds., Acid sulfate weathering, Soil Science Society of America Special Publication 10, p. 37-57.
Nordstrom, D.K., Jenne, E.A., and Ball, J.W., 1979, Redox equilibria of iron in acid mine waters, *in* Jenne, E.A., ed., Chemical modeling in aqueous systems, American Chemical Society Symposium Series 93, p. 51-79.

Odum, J.K., Hauff, P.L., and Farrow, R.A., 1982, A new occurrence of ammoniumjarosite in Buffalo, Wyoming: Canadian Mineralogist, v. 20, p. 91-95.
Palache, C., Berman, H., and Frondel, C., 1951, Dana's system of mineralogy, v. 2, John Wiley, New York, 1124 p.
Parfitt, R.L., Atkinson, R.J., and Smart, R. St.C., 1975, The mechanism of phosphate fixation by iron oxides: Soil Science of America Proceedings, vol. 39, p. 837-841.
Princeton Gamma-Tech, Inc., 1994, Integrated microanalyzer for imaging and X-ray software manual, v. 7. Princeton, N.J.
Ripmeester, J.A., and Ratcliffe, C.I., 1986, Hydronium ion in the alunite-jarosite group: Canadian Mineralogist, v. 24, p. 435-447.
Schulze, D.G., and Schwertmann, U., 1984, The influence of aluminum on iron oxides: X. Properties of Al-substituted goethite: Clay Minerals, vol. 19, p. 521-539.
Sclar, C.B., 1961, Decomposition of pyritized carbonaceous shale to halotrichite and melanterite: American Mineralogist, v. 46, p. 754-756.
Shayan A., and Lancuki, C.J., 1984, Rapid decay of slate roofing tiles in service: Abstracts of the Geological Society of Australia, v. 12, p. 479.
Trumpf, W.F., Morgan, E.L., and Herrmann, Ray, 1979, Man induced acid drainage impact on benthic macroinvertebrate communities in the Great Smoky Mountains National Park: *in* Lin, R.M., ed., Proceedings of the First Conference on Scientific Research in the National Parks, U.S. Department of the Interior, National Park Service Transactions and Proceedings Series Number 5, v. I, p. 643-647.
Turner, L.J., and Kramer, J.R., 1991, Sulfate ion binding on goethite and hematite: Soil Science, vol. 152, p. 226-230.
Wiese, R.G., Jr., Powell, M.A., and Fyfe, W.S., 1987, Spontaneous formation of hydrated iron sulfates on laboratory samples of pyrite- and marcasite-bearing coals: Chemical Geology, v. 63, p. 29-38.
Young, B., and Nancarrow, P.H.A., 1988, Rozenite and other sulphate minerals from the Cumbrian coalfield: Mineralogical Magazine, v. 52, p. 551-552.
Zodrow, E.L., 1980, Hydrated sulfates from Sydney Coalfield, Cape Breton Island, Nova Scotia, Canada: the copiapite group: American Mineralogist, v. 65., p. 961-967.

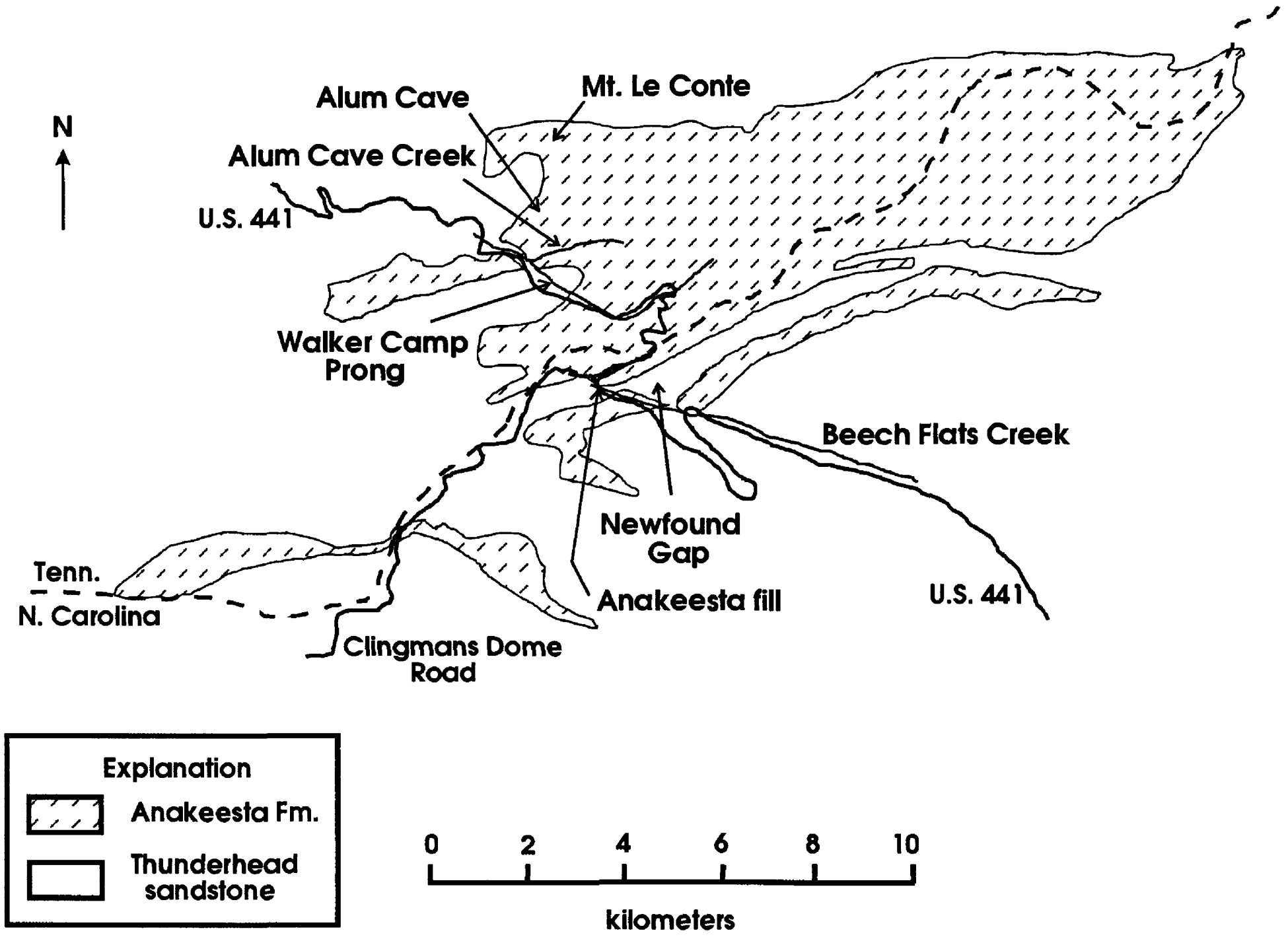

Figure. 1. Sketch map of the central part of the Great Smoky Mountains National Park that shows the location of Alum Cave and exposures of Anakeesta Fm. After Hadley and Goldsmith, 1963; Herrmann and others, 1979.

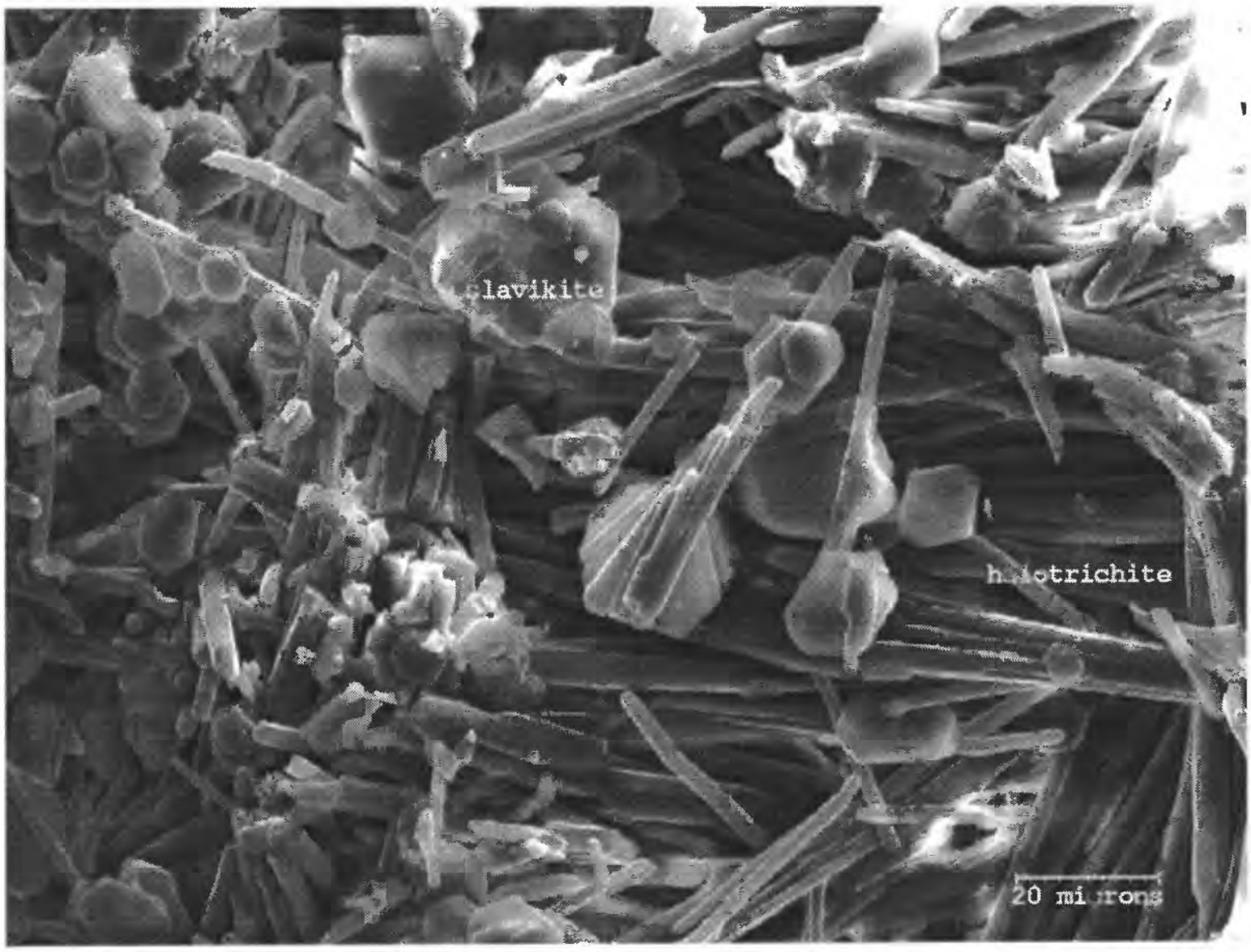

Figure 2a. Aggregate of fine halotrichite needles and euhedral hexagonal tabular grains of slavikite. Secondary electron image.

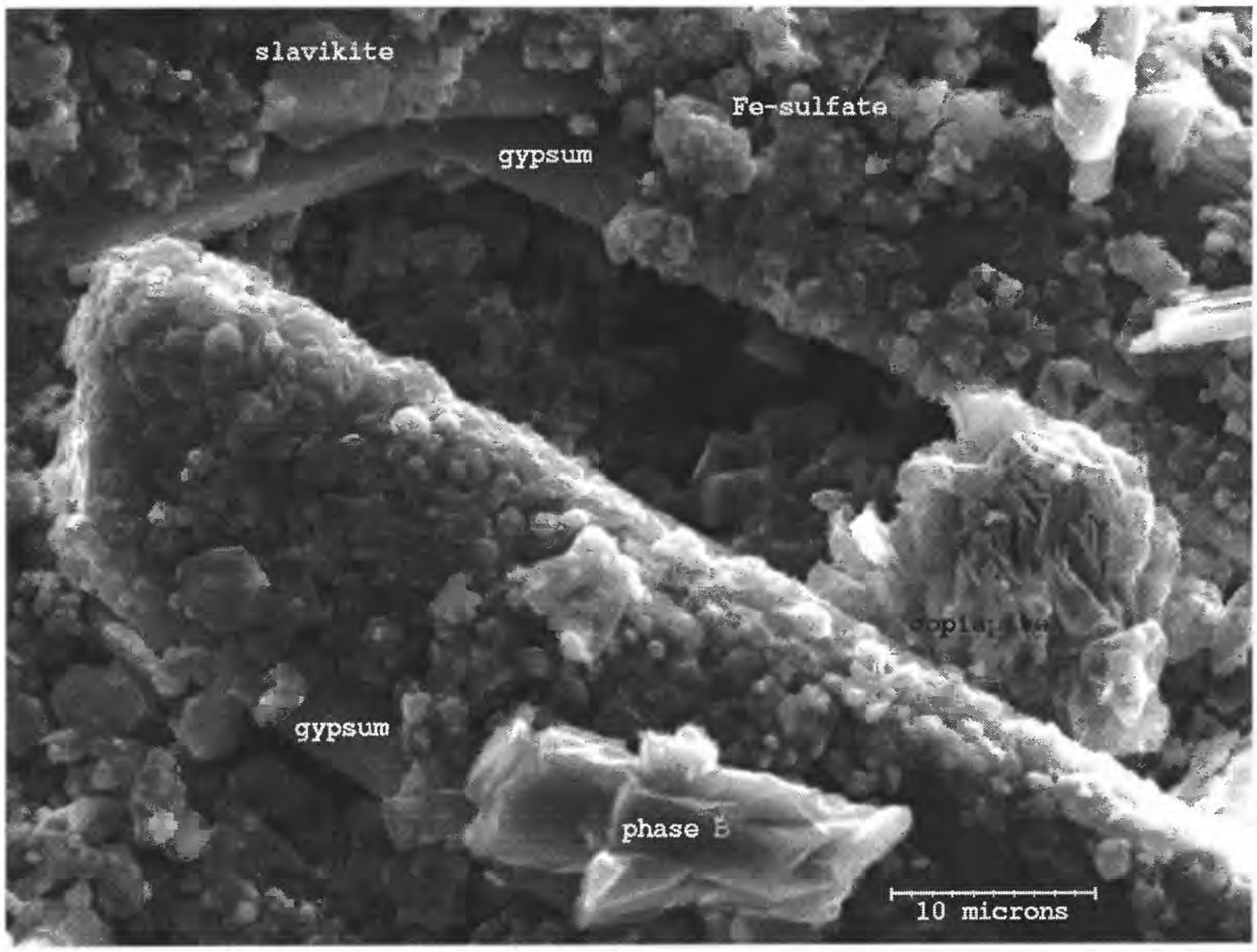

Figure 2b. Encrustation of secondary minerals on phyllite surface. Tabular grains of gypsum are encrusted with globular masses of Fe-sulfate, probably rozenite, or, possibly, melanterite, although melanterite has not been identified by XRD in the copiapite-bearing sampling. Nodular rosettes of copiapite and euhedral grains of slavikite and phase B, tentatively identified as an Fe-sulfate, are also present. Secondary electron image.

Figure 3a. Thin Fe-rich red crust with a botryoidal habit that coats phyllite. The crust is probably poorly crystalline goethite. Euhedral grains of phase A, tentatively identified as hydronium jarosite, partly encrust the red crust. Secondary electron image.

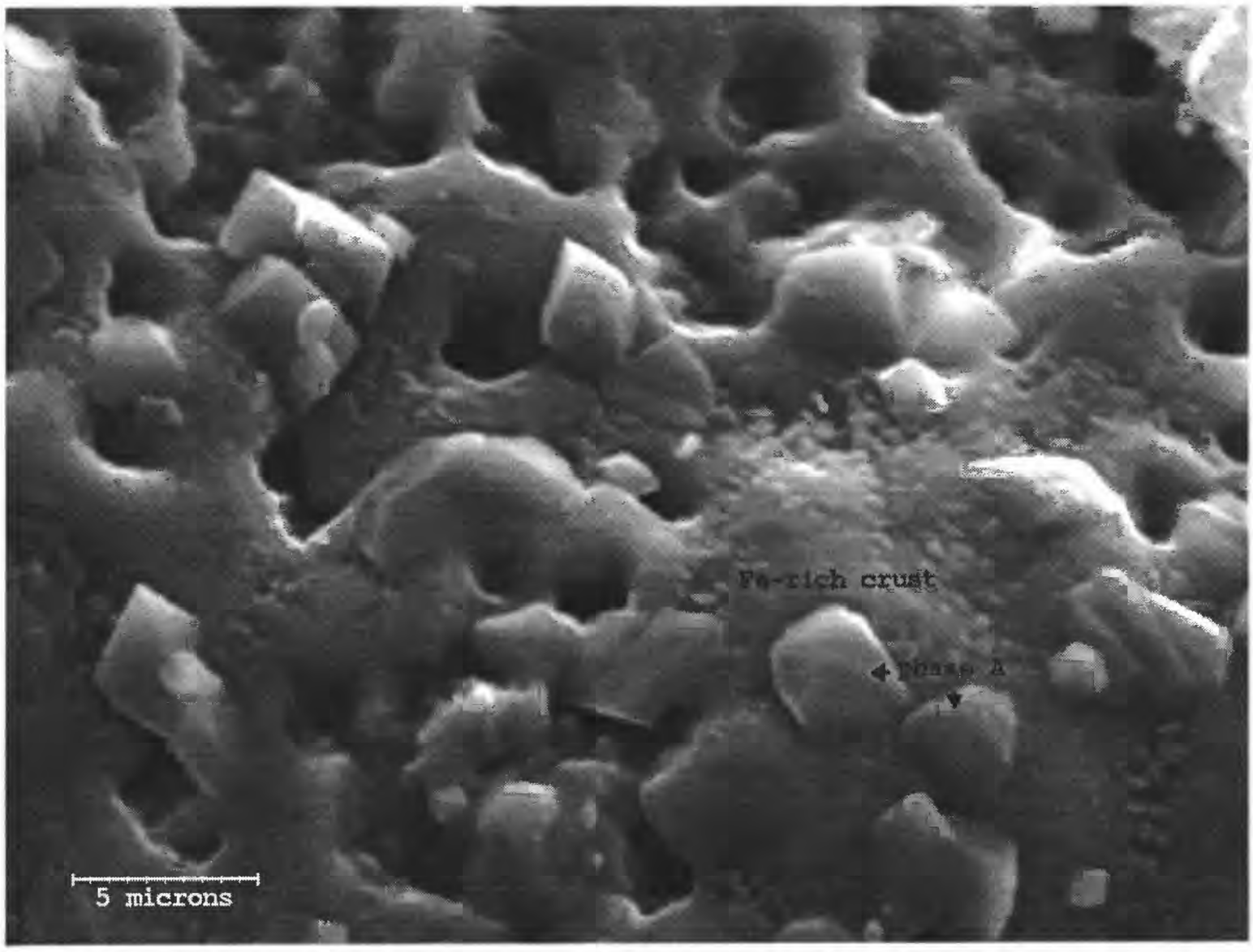

Figure 3b. Thin Fe-rich red crust with a "swiss-cheese" texture that SEM-EDS analysis indicates is compositionally similar to the botryoidal crust (poorly crystalline goethite) shown in Figure 3a. The surface of the crust has a fine texture and is not smooth. Grains of phase A, suspected hydronium jarosite, are sparsely distributed over the surface. Secondary electron image.

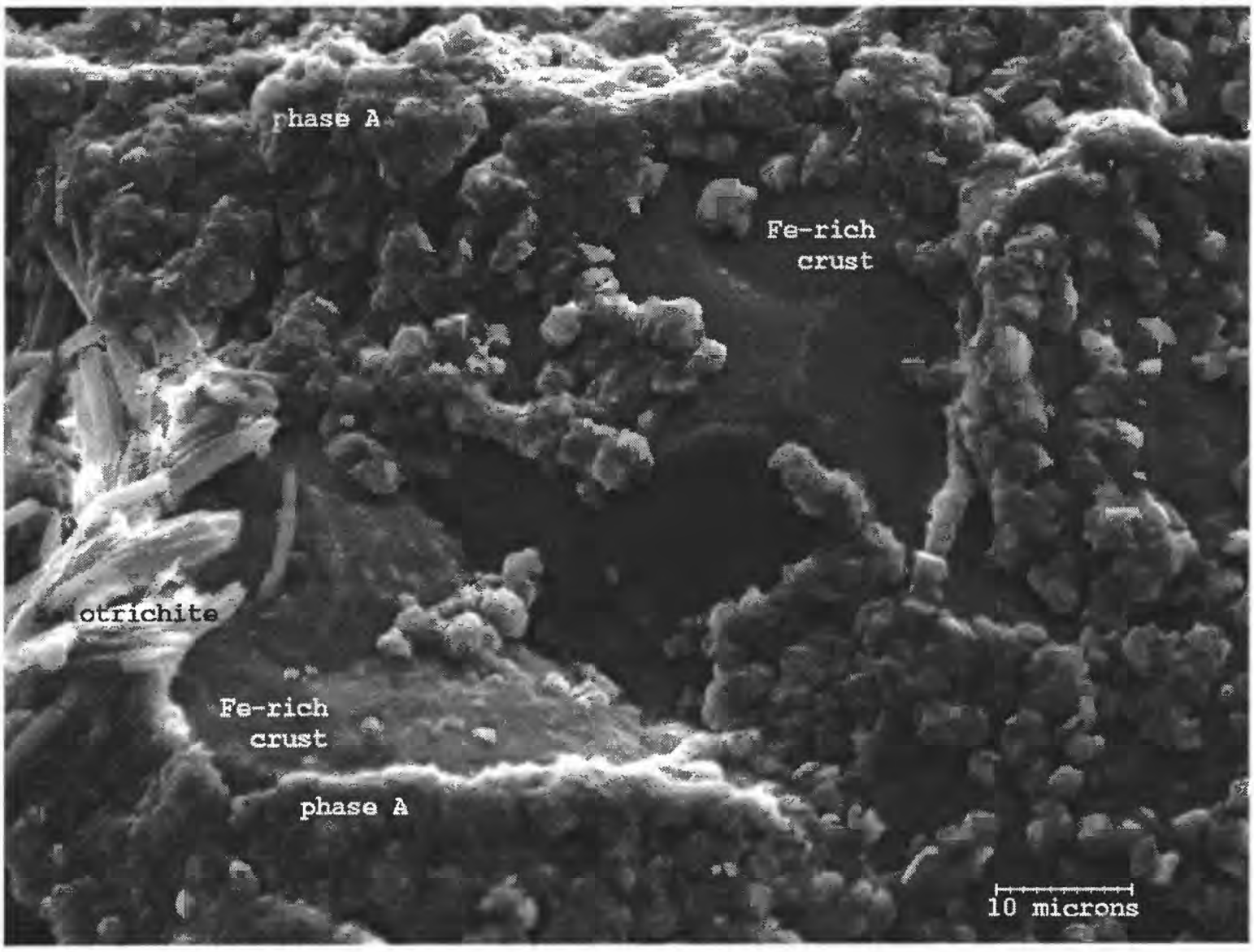

Figure 3c. Massive encrustation of phase A, suspected hydronium jarosite, on thin Fe-rich red crust (poorly crystalline goethite). Phase A forms grains only a few microns across. A small spray of halotrichite needles is also present. Secondary electron image.

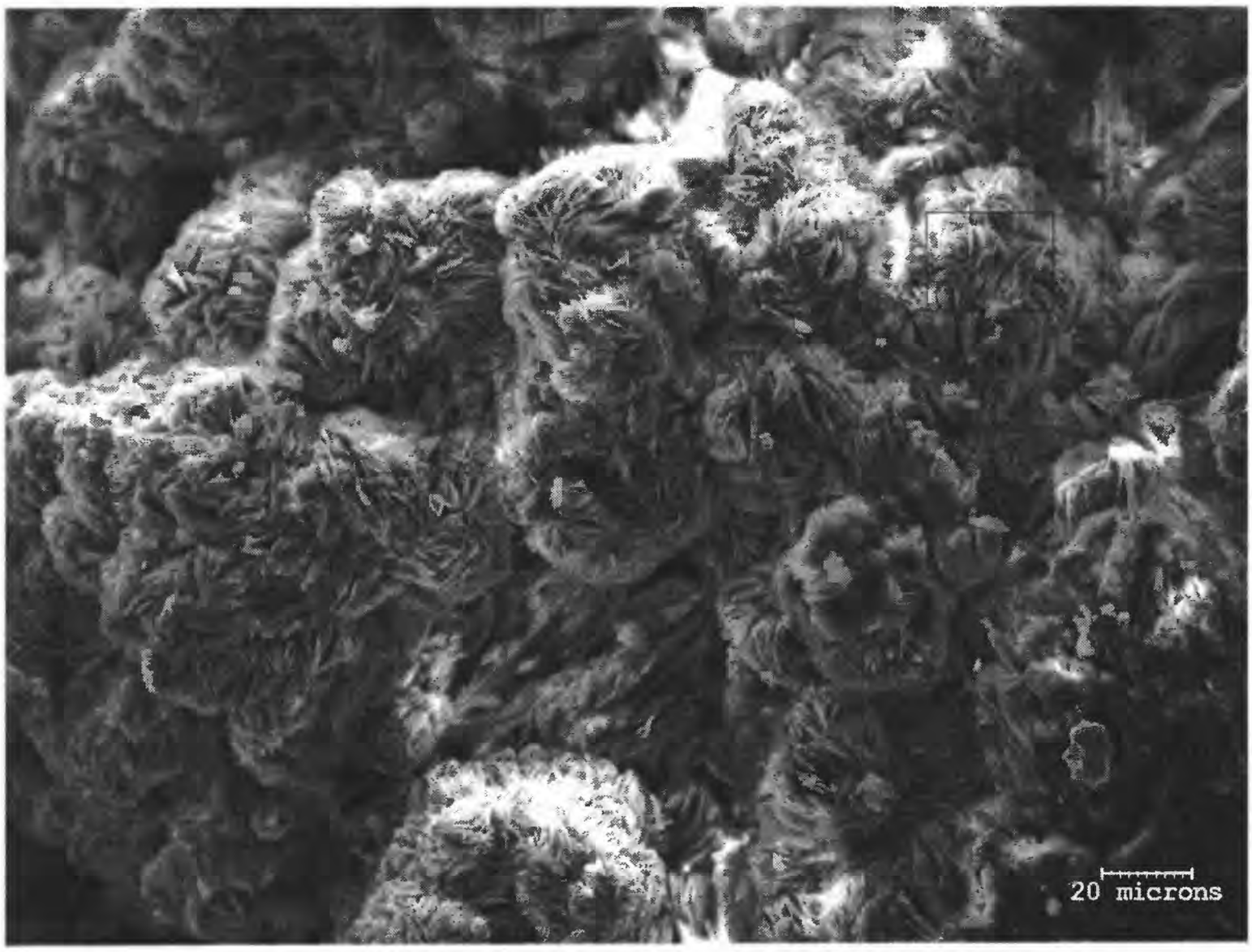

Figure 4a. Thick nodular encrustation of copiapite on phyllite. Boxed area (upper right quadrant) is the area shown in Figure 4b. Secondary electron image.

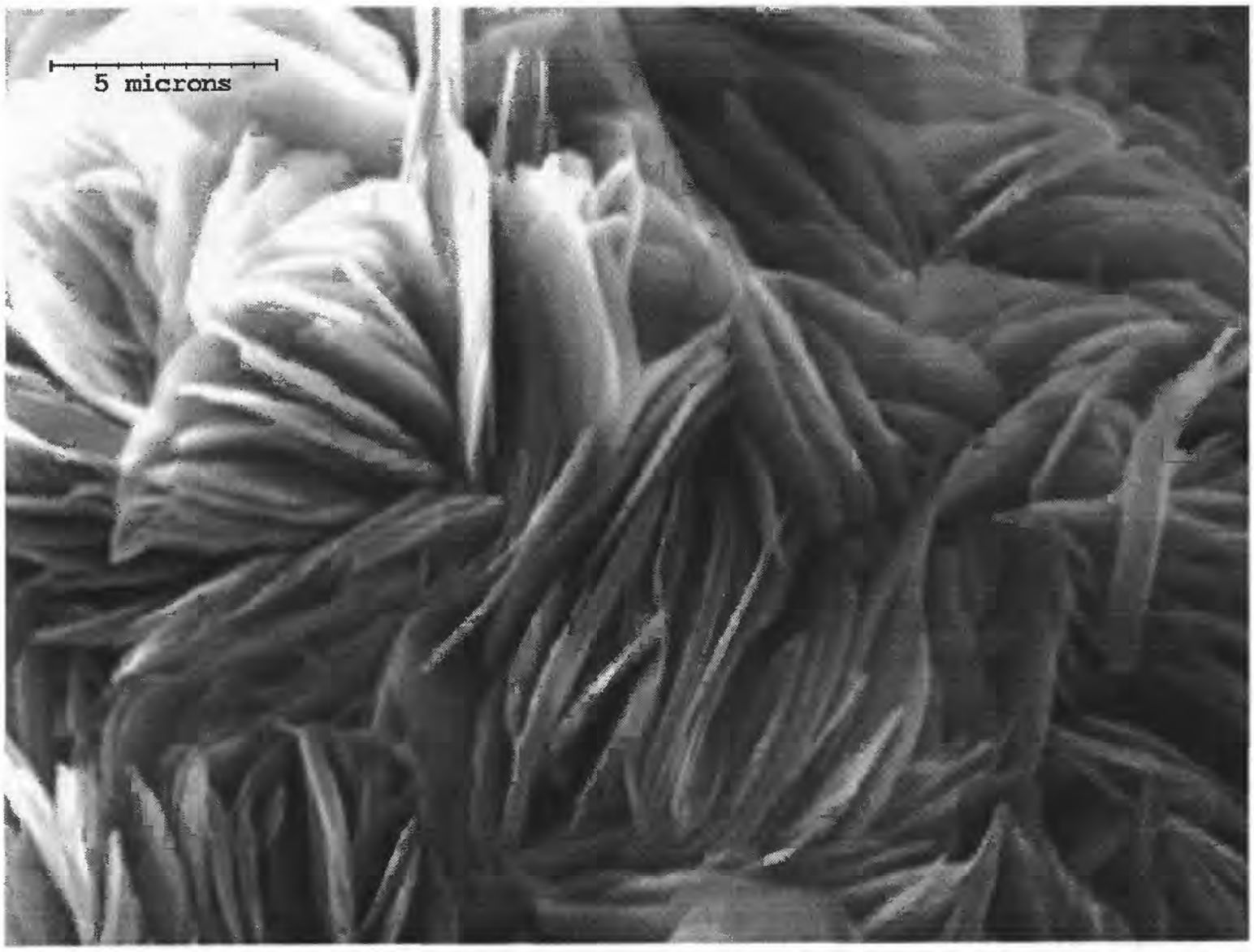

Figure 4b. High magnification image of the boxed area shown in Figure 4a. The nodules or rosettes shown in Figure 4a are composed of thin tabular grains of copiapite. Secondary electron image.

Table 1. Ideal chemical formulas of metamorphic minerals from phyllite, Anakeesta Formation, Alum Cave, Great Smoky Mountains National Park

Mineral	Ideal formula
Major constituents	
quartz	SiO_2
muscovite	$KAl_2(Si_3Al)O_{10}(OH,F)_2$
paragonite	$NaAl_2(Si_3Al)O_{10}(OH)_2$
chlorite	$(Mg,Fe^{+2},Mn)_5Al(Si_3Al)O_{10}(OH)_8$
Accessory minerals	
graphite	C
garnet	$(Mn,Fe^{+2},Mg,Ca)_3Al_2(SiO_4)_3$
zircon	$ZrSiO_4$
allanite	$(Ce,Ca,La,Mn)_2(Fe^{+2},Fe^{+3},Al)_3(SiO_4)_3(OH)$
rutile	TiO_2
pyrite	FeS_2
pyrrhotite	$Fe_{(1-x)}S$, $(x=0\text{-}0.17)$
apatite	$CaPO_4$
monazite	$(Ce,La,Nd,Th)PO_4$
xenotime[1]	YPO_4

[1]tentative identification

Table 2. Characteristics of secondary minerals from the Anakeesta Formation, Alum Cave, Great Smoky Mountains National Park

Sulfate minerals that form thick encrustations

Mineral	Ideal Formula	Textural characteristics	Chemical characteristics
alunogen	$Al_2(SO_4)_3 \cdot 17H_2O$	white massive encrustations; associated with slavikite	no detectable cation substitutions
copiapite	$Fe^{2+}Fe_4^{3+}(SO_4)_6(OH)_2 \cdot 20H_2O$	yellow "nodular" encrustations (Fig. 4a); "nodules" are rosettes of thin (< 1 μm thick) tabular grains (Fig. 4b); also associated with other secondary minerals (Fig. 2b)	minor P, Mg, Al detected
gypsum	$CaSO_4 \cdot 2H_2O$	aggregates of colorless to white laths up to ~100 μm long x 20-30 μm wide (Fig. 2b); thin colorless plates	no detectable cation substitutions
halotrichite-pickeringite	$Fe^{2+}Al_2(SO_4)_4 \cdot 22H_2O$ - $MgAl_2(SO_4)_4 \cdot 22H_2O$	fine, nodular, or botryoidal aggregates of needles (Fig. 2a) and thin (< 3 μm thick) laths, up to 450 μm long, or as more massive encrustations; color ranges from white or nearly colorless through various shades of tan, yellow, pink-tan, medium pink to pink-orange	white to nearly colorless needles appear richer in Mg than the more colored varieties that contain more Fe; minor Mn (< 2 wt% MnO) present in all varieties, with the greatest concentrations of Mn usually present in the relatively darker colored varieties; Zn (estimated at < 0.5 wt% ZnO) detected
melanterite	$Fe^{2+}SO_4 \cdot 7H_2O$	globular efflorescence forms nearly pure white encrustations; grains are < 5 μm across	minor Mg detected in all occurrences plus Mn in some occurrences

Table 2. Characteristics of secondary minerals --Continued

Mineral	Ideal formula	Textural characteristics	Chemical characteristics
rozenite	$Fe^{2+}SO_4 \bullet 4H_2O$	globular efflorescence forms creamy white encrustations, grains are <5 μm across	minor Mg detected in all occurrences plus Mn in some occurrences
slavikite[1]	$MgFe_3(SO_4)_4(OH)_3 \bullet 18H_2O$	hexagonal tabular grains, <25 μm across; forms green-yellow encrustation on phyllite and occurs with halotrichite (Fig. 2a)	minor Mn, Al detected
epsomite[2]	$MgSO_4 \bullet 7H_2O$	rounded gains, <60 μm across, associated with Mg-rich halotrichite; uncommon	no detectable cation substitutions
starkeyite[2]	$MgSO_4 \bullet 4H_2O$	aggregates rounded rod-like to grains form milky white encrustation; uncommon	minor Fe detected
phase B (Fe-sulfate?)	unknown	tabular grains <20 μm long x <10 μm wide (Fig. 2b); also forms encrusting masses of tabular grains that coat phyllite; uncommon	Fe + S + minor Mg detected

Associated with sulfate minerals that form encrustations

goethite	FeO(OH)	black to black-red grains embedded in aggregates of other secondary minerals; fresh fractured surface is smooth as observed in the SEM; exposed surfaces are partly encrusted with grains of phase A	minor Si, Al, P; proportions of the minor elements are not consistent among goethite from different samples or from goethite from different areas of the same sample; minor S also detected on exposed surfaces

Table 2. Characteristics of secondary minerals --Continued

Thin oxidized crusts

Mineral	Ideal formula	Textural characteristics	Chemical characteristics
Fe-rich crusts (probably poorly crystalline goethite)	FeO(OH) (goethite)	red crusts on phyllite - textures as observed by SEM: (a) smooth and fractured; (b) botryoidal (Fig. 3a); (c) "swiss-cheese" textured (Fig. 3b); all varieties are sparsely to heavily encrusted by phase A (Figs. 3a, 3b, 3c)	(a, b, c) Fe + minor S + lesser amounts of P, Si, Al detected
phase A (hydronium jarosite?)	$(H_3O)Fe_3^{+3}(SO_4)_2(OH)_6$ (hydronium jarosite)	euhedral-subhedral grains, <5 μm across (Figs. 3a, 3b, 3c); (pseudo?)cubic to rhombohedral morphology	only Fe + S detected

[1]formula of slavikite as reported by Makovický and Streško (1967); SEM-EDS and standardless analysis are consistent with this formula rather than the formula [$NaMg_2Fe_5^{3+}(SO_4)_7(OH)_6 \bullet 33H_2O$] reported by Fleischer and Mandarino (1991).
[2]see text for discussion of the tentative identification of these minerals.

Table 3. Summary of the secondary minerals identified in samples of phyllite, Anakeesta Formation, Alum Cave, Great Smoky Mountains National Park [+, mineral present; -, mineral absent or not found]

Mineral	Sample ACA-1C-1	ACA-1D	ACA-1E
alunogen	-	+	+
copiapite	-	-	+
Fe-rich red crust(s)	+	+	+
goethite	+	+	+
gypsum	+	-	+
halotrichite[1]	+	+	+
melanterite	+	+	-
rozenite	+	+	+
slavikite	+	+	+
epsomite	-	-	+
starkeyite	-	-	+
phase A	+	+	+
phase B	-	-	+

[1]includes all compositional varieties of halotrichite and halotrichite-pickeringite solid solution (see Table 1)